PHILOSOPHICAL TRANSACTIONS A

royalsocietypublishing.org/journal/rsta

Review

Cite this article: Levi M. 2019 Geometrical aspects of rapid vibrations and rotations. *Phil. Trans. R. Soc. A* **377**: 20190014.
http://dx.doi.org/10.1098/rsta.2019.0014

Accepted: 8 August 2019

One contribution of 11 to a theme issue 'Topological and geometrical aspects of mass and vortex dynamics'.

Subject Areas:
differential equations

Keywords:
normal form, Lorentz force, ponderomotive magnetism

Author for correspondence:
Mark Levi
e-mail: levi@math.psu.edu

THE ROYAL SOCIETY PUBLISHING

Geometrical aspects of rapid vibrations and rotations

Mark Levi

Department of Mathematics, Pennsylvania State University, University Park, PA 16802-1800, USA

ML, 0000-0001-6345-9079

The counterintuitive phenomenon of stabilization of the inverted pendulum by the vertical vibration of its pivot has been known for over a century. This remarkable effect attracted attention of many mathematicians and physicists, including Kapitsa, Feynman, Arnold, Moser and others. The 1989 Nobel Prize in Physics was awarded to W. Paul for his discovery of the particle trap based on this phenomenon. The inverted pendulum is a tip of an 'iceberg' of related phenomena arising in systems with high-frequency time-dependence. This article surveys some related phenomena discovered more recently, some connections with differential geometry and mechanics, and some new geometrical insights.

This article is part of the theme issue 'Topological and geometrical aspects of mass and vortex dynamics'.

1. The Stephenson–Kapitsa effect

(a) A geometrical explanation of the effect

This section describes the first motivating example of the group of phenomena described in this brief survey: the so-called Kapitsa pendulum—the effect was actually discovered by Stephenson [1] in 1908, decades before Kapitsa's paper [2] appeared. If the pivot of the pendulum—a mass on a stick—is made to oscillate vertically with sufficiently high frequency then the upside-down position becomes stable. This effect fascinated many mathematicians and physicists; both Arnold and Moser demonstrated this effect in their lectures. This problem was analysed in numerous papers [3–9] and described in some famous texts, e.g. Feynman's [10] and Arnold's [11]. The Stephenson–Kapitsa effect led also to the invention of the cyclotron [12] and of the Paul trap, for which W. Paul received Nobel Prize in physics in 1989.

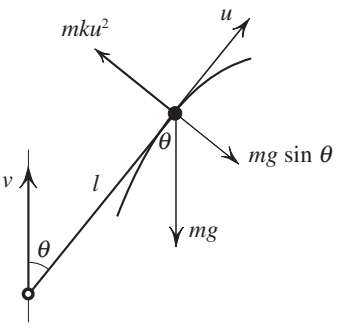

Figure 1. A geometrical explanation of the stabilization effect for the simple pendulum.

For almost 90 years since its 1908 discovery by Stephenson, all the studies of the stabilization phenomenon were analytical, usually based on averaging theory/normal form reduction, until a simple geometric explanation was found [13]; we begin by describing this idea.

(i) Kapitsa's effect and the curvature of the tractrix

Figure 1 shows an inverted pendulum (a weightless rod with a point mass at the end) whose pivot P is vibrated in the vertical direction with a small amplitude but with high frequency which produces a great acceleration. The point mass is subject to great force due to violent acceleration of the pivot; *this force is directed along the rod.* So if, as a thought experiment, we constrain the velocity of the point mass to the direction of the rod, we will not interfere with this large force. On the other hand, the mass thus constrained will oscillate along an arc of a pursuit curve (the tractrix), as illustrated in figure 1. Therefore, the mass will push against the constraint with the centrifugal force mku^2 (figure 1). And this suggests that *removing the constraint (not there in the first place) will let the particle behave as if it were subject to this centrifugal force* mku^2 (figure 1). This is a heuristic explanation of stabilization by vibration. To make this explanation quantitative, let us compute the stabilizing centrifugal force over the period of oscillation of the pivot, and then take its average over the period of pivot's oscillation. The force is (setting the mass $m=1$)

$$ku^2 = k(v\cos\theta)^2, \tag{1.1}$$

where $k=k(\theta)$ is the curvature of the tractrix. Substituting $k=l^{-1}\tan\theta$ (skipping the simple derivation) into (1.1) yields $(v^2/l)\sin\theta\cos\theta$ for the centrifugal force of the non-existent constraint. This suggests that the vibrated pendulum behaves as if subject to the additional force

$$\frac{\overline{v^2}}{l}\sin\theta\cos\theta, \tag{1.2}$$

where the bar denotes the time average. This leads to a cautious guess that the pendulum will be upside-down stable if this stabilizing force exceeds the destabilizing component of gravity:

$$\frac{\overline{v^2}}{l}\sin\theta\cos\theta > g\sin\theta.$$

In the limit of small θ this amounts to

$$\frac{\overline{v^2}}{l} > g, \tag{1.3}$$

a linearized stability criterion, so far unproven in this heuristic discussion. It should be added that this criterion is asymptotic: it guarantees stability only under the above-stated assumption of sufficiently high frequency producing sufficiently high acceleration; the term 'sufficient' is made more precise in theorem 2.1 in the next section.

Although no mention of differential equations has been made, we obtained some specific statements about differential equations—the statements that turn out to be correct, but that take several pages to prove rigorously. Let us summarize two of these results (linearized version of this discussion can be found in [13]).

1. Note first that the differential equation for angle θ of the pendulum in figure 1 is
$$l\ddot{\theta} + (-g - a(t))\sin\theta = 0, \tag{1.4}$$
where $a = \dot{v}$ is the pivot's acceleration. The derivation of (1.4) is given at the end of this section. The above heuristic discussion suggests that the effect of the pivot's vibration can be replaced (to the leading order) by the restoring centrifugal force (1.2); and the angle φ of the mathematical pendulum subject to this force, in addition to the gravity, is governed by Newton's Second Law projected onto the tangent direction to the circle
$$\underbrace{\frac{\mathrm{d}^2}{\mathrm{d}t^2}(l\varphi)}_{m\cdot\text{acceleration}} = \underbrace{g\sin\varphi}_{\text{destabilizing force}} \underbrace{-\frac{\overline{v^2}}{l}\sin\varphi\cos\varphi}_{\text{stabilizing force}}, \tag{1.5}$$
to the leading order. It takes several pages to prove that this averaged equation (1.5) is correct [13], although it only took a few lines to derive it heuristically. Theorem 2.1 in the next section contains a precise statement, and the details of the proof can be found in [13].
2. Consider the linearization of (1.4) at the top equilibrium:
$$l\ddot{\theta} + (-g - a(t))\theta = 0; \tag{1.6}$$
we kept the same notation for θ. Assume the high frequency and small amplitude vibration, e.g. $a(t,\omega) = \omega^\beta A(\omega t)$, where A is periodic of zero average, ω is large, and where $\beta < 2$ to assure small amplitude. As is well known, stability of (1.6) is equivalent to Floquet matrix F satisfying the ellipticity condition
$$|\mathrm{tr}\, F| < 2. \tag{1.7}$$
It is remarkable that this algebraic condition (1.7) admits (under the asymptotic assumptions stated at the outset) a physical interpretation of the centrifugal force exceeding the gravitational force in the sense of (1.3). This is a symptom of a previously hidden role of geometry in averaging theory. Some recent progress in exploring this connection will be outlined in this brief survey.

Example. High frequency and small amplitude *do not automatically guarantee stability:* stabilization must be strong enough to overcome the destabilization, in the sense of (1.3). As an example, with $l = 1, g = 1$ and $a = \omega\sin\omega t$ (high acceleration, high frequency, small amplitude) the condition (1.3) fails, and with it does stability, no matter how large ω is: the centrifugal force of the fictitious constraint in figure 1 is too weak to overcome gravity. Intuitively, the mean square velocity $\overline{v^2}$ is not high enough.

Let us, therefore, increase the acceleration (and thus the velocity), keeping the same frequency—take, for instance, $a = \omega^{3/2}\sin\omega t$. The choice of power guarantees that the amplitude is still small, namely $\omega^{-1/2}$ (but not as small (ω^{-1}) as in the preceding example of instability; this increase is unavoidable since we kept the frequency and increased the acceleration). The stability criterion (1.3) now becomes
$$\frac{\omega}{2l} > g, \quad \text{or } \omega > 2gl.$$
Our heuristic discussion relied on the asymptotic assumption of high frequency and high acceleration, and so an earlier remark applies here: this condition alone does not guarantee stability without the additional assumption of large ω. A numerical computation in the present example shows that for $l = 1, g = 1$ stability begins not at $\omega_0 = 2gl = 2$, but rather at $\omega = 2.3199\ldots$, higher than the asymptotic criterion requires.

(ii) Derivation of the vibrated pendulum equation (1.6)

Starting with the standard pendulum with constant gravity $g = \text{const.}$, the tangential acceleration is given by the tangential component of the gravity, referring to figure 1; by Newton's Second Law projected onto the tangent to the circle at θ we have

$$m\frac{\mathrm{d}^2}{\mathrm{d}t^2}(l\theta) = mg\sin\theta. \tag{1.8}$$

Now we let the pivot undergo acceleration $a = a(t)$ in the vertical direction. In the accelerating frame of the pivot, the acceleration gives rise to the D'Alembert inertial force $-ma(t)$ acting on the pendulum, pointing vertically down if $a > 0$ and up if $a < 0$. The acceleration thus can equivalently be replaced by the variable gravity, $-g - a$ instead of the former $-g$. Making this replacement in (1.8) gives

$$l\ddot{\theta} = (g + a)\sin\theta.$$

And the linearization at the equilibrium $\theta = 0$ gives (1.6).

(b) Curvature of the tractrix in averaged Hill's equations

The geometrical observation just discussed leads to the following related observation: *curvature of the tractrix shows up in averaging Hill's equation*

$$\ddot{x} + q(t,\varepsilon)x = 0, \quad \langle q\rangle = 0 \tag{1.9}$$

with $q(t,\varepsilon) = \varepsilon^\alpha A(t/\varepsilon)$, where $\alpha > -2$ and $A(\tau + 1) = A(\tau)$ and where we take $\langle A\rangle = 0$.

Indeed, according to the above observation and theorem 4.2 below the truncated averaged system is

$$\ddot{X} + \kappa\langle v^2\rangle X = 0, \tag{1.10}$$

where $\kappa = k'(0)$, $k(x) =$ curvature of the tractrix generated by unit segments ($\ell = 1$).

(c) Asymptotics of path integrals and curvature

As yet another consequence of the discussion in §1a, the curvature of the tractrix is seen to arise in a problem of composition of non-commuting matrices from $SL(2,\mathbb{R})$. Indeed, Hill's equation (1.9) can be written in the Hamiltonian form

$$\dot{\mathbf{x}} = A(t,\varepsilon)\mathbf{x}, \quad \mathbf{x}\in\mathbb{R}^2,\ A = \begin{pmatrix} 0 & 1 \\ -q & 0 \end{pmatrix}.$$

Now the fundamental solution matrix $F(t)$ is given by $P\exp\int_0^t A(\tau,\varepsilon)\mathrm{d}\tau$, where the path integral $P\exp$ is defined as the limit of a product of a family of non-commuting 2×2 matrices of the form $I + A\,\mathrm{d}\tau$, namely

$$F(t) = \lim_{n\to\infty}\big(I + A(t_n)\Delta t\big)\big(I + A(t_{n-1})\Delta t\big)\ldots\big(I + A(t_1)\Delta t\big),$$

where $\Delta t = t/n$ and $t_k = (k/n)t$. According to the preceding section, the leading term in the asymptotic expression for this product is

$$F = \exp\begin{pmatrix} 0 & 1 \\ -\kappa\langle v^2\rangle & 0 \end{pmatrix} + \ldots,$$

and the term $-\kappa\langle v^2\rangle$ has a physical interpretation in terms of centrifugal acceleration of the motion along a tractrix.

2. Averaging of oscillatory systems: analytical approach

In this section, we state an averaging theorem in the algebraic form and then illustrate its geometrical side on several examples. Further details and proofs can be found in [13].

(a) The result

The linearized pendulum equation (1.6), or its nonlinear counterpart $l\ddot{x} + (-g - a(t))\sin x = 0$ are special cases of the system

$$\ddot{\mathbf{x}} = a(t,\varepsilon)\mathbf{f}(\mathbf{x}); \tag{2.1}$$

here $\mathbf{f}: \mathbb{R}^n \to \mathbb{R}^n$. We take a to be 'large and fast':

$$a(t,\varepsilon) = \varepsilon^\alpha A\left(\frac{t}{\varepsilon}\right), \quad \text{with } \alpha > -2, \tag{2.2}$$

where $A(\tau+1) = A(\tau) = O(1)$ and $\varepsilon \ll 1$. We note that under this assumption the acceleration is allowed to be very large, but the 'displacement' $s(t,\epsilon)$ is small:

$$s(t,\varepsilon) = \int_{t_0}^{t}\int_{\tau_0}^{\tau} (a(s) - \langle a\rangle)\,\mathrm{d}s\mathrm{d}\tau \sim \varepsilon^{2+\alpha} \ll 1; \tag{2.3}$$

here t_0, τ_0 are chosen so that the integral is a periodic function with zero average.

We are thus dealing with high-frequency violent vibrations. Unless stated otherwise, we always assume that $\mathbf{f}$ is real analytic, although $C^{(5)}$ actually suffices for the next result.

Theorem 2.1 ([13]). *Under the scaling assumption* (2.2) *the system* (2.1) *reduces to the averaged equation*

$$\ddot{\mathbf{X}} = \langle a\rangle \mathbf{f}(\mathbf{X}) - \langle v^2\rangle \mathbf{f}'(\mathbf{X})\mathbf{f}(\mathbf{X}) + \mathbf{E}, \tag{2.4}$$

where[1]

$$v = \int_{t_0}^{t} (a - \langle a\rangle)\,\mathrm{d}t, \quad \langle v\rangle = 0 \tag{2.5}$$

and where $|\mathbf{E}| \le M\varepsilon^{3+5\alpha/2}$ *with* $M > 0$ *depending on* $\mathbf{f}$ *and* A *but not on* ε, *via the transformation* $\mathbf{x} = \mathbf{X} + s(t,\varepsilon)\mathbf{f}(\mathbf{X}) + O(\varepsilon)$, *where* s *was defined in* (2.3)

We note that $\mathbf{f}'\mathbf{f}$ has the interpretation of the acceleration of the particle carried by the velocity field $\mathbf{f}$, the so-called convective acceleration. In the solid mechanics literature the notation $(\mathbf{f}\cdot\nabla)\mathbf{f}$ is used.

The formal derivation of the averaged equation (2.4) can be found in [2,14], or obtained by reducing (2.1) to a first-order system and using the standard method of normal form, e.g. [15]. A detailed proof of theorem 2.1 with estimates can be found in [13].

(b) Application 1: unit vectorfields in $\mathbb{R}^n$

In this case, the geometry becomes particularly transparent: if $|\mathbf{f}(\mathbf{x})| \equiv 1$, then equation (2.4) is equivalent to

$$\ddot{\mathbf{X}} = \langle a\rangle\ \mathbf{f}(\mathbf{X}) - k\ \langle v^2\rangle\ \mathbf{n} + \mathbf{E}, \tag{2.6}$$

where $\mathbf{n}(\mathbf{x})$ is the principal unit normal vector to the integral curve of $\mathbf{f}$ at $\mathbf{x}$ and where $k(\mathbf{x})$ is the curvature of this curve. $\mathbf{E}$ satisfies the same estimate as above.

Observe that $-kv^2\mathbf{n}$ is precisely the centrifugal force acting on a bead of unit mass sliding along a curve of curvature k with speed v.

Proof of (2.6) follows at once from (2.4) by application of the following observation.

[1] $\mathbf{f}'(\mathbf{x})$ denotes the Jacobian $n \times n$ matrix of partial derivatives.

Lemma 2.2 ([13]). *In a vector field of unit vectors*: $|\mathbf{f}(\mathbf{x})| = 1$, $\forall \mathbf{x}$, *the curvature* $k = k(\mathbf{x})$ *and the principal unit normal* $\mathbf{n} = \mathbf{n}(\mathbf{x})$ *to the integral line through* $\mathbf{x}$ *are given by*

$$k\,\mathbf{n} = \mathbf{f}'\mathbf{f} \equiv (\mathbf{f}\cdot\nabla)\mathbf{f}. \tag{2.7}$$

Proof of the lemma. Let $\mathbf{x} = \mathbf{x}(s)$ be an integral curve: $(\mathrm{d}\mathbf{x}(s))/(\mathrm{d}s) = \mathbf{f}(\mathbf{x}(s))$ since $|\mathbf{f}| \equiv 1$, s is the arc length parameter. Thus

$$k\mathbf{n} \overset{\text{def}}{=} \frac{\mathrm{d}^2\mathbf{x}}{\mathrm{d}s^2} = \frac{\mathrm{d}}{\mathrm{d}s}\,\mathbf{f}(\mathbf{x}(s)) = \mathbf{f}'(\mathbf{x})\mathbf{f}(\mathbf{x}),$$

as claimed. ∎

In the special case $\mathbf{x} \in \mathbb{R}^2$ equation (2.6) becomes

$$\ddot{\mathbf{X}} = \langle a\rangle \mathbf{f}(\mathbf{X}) - \langle v^2\rangle \operatorname{curl}\mathbf{f}\cdot\mathbf{n} + \mathbf{E}, \tag{2.8}$$

where curl denotes the two-dimensional (scalar) curl. This result follows from the following simple observation.

Lemma 2.3 ([13]). *The curvature* $k(\mathbf{x})$ *of trajectories of a unit vectorfield* $\mathbf{f}(\mathbf{x}) \equiv 1$ *in* $\mathbb{R}^2$ *coincides with the (scalar) curl*:

$$\mathit{curl}\ \mathbf{f}(\mathbf{x}) = k(\mathbf{x}), \tag{2.9}$$

where the sign of k *is decided by the definition of the curvature:* $k = (\mathrm{d}\theta)/(\mathrm{d}s)$, *with the direction of increasing* s *given by* $\mathbf{f}$.

Proof of Lemma 2.3. By the definition, the curl in 2D is the sum of the angular velocities of two infinitesimal segments A and B orthogonal to each other at $\mathbf{x}$ as these segments are carried with the flow: $\operatorname{curl}\mathbf{f} = \omega(A) + \omega(B)$. Take one of these segments A to be tangent to the trajectory at $\mathbf{x}$, so that $B \perp A$ at $\mathbf{x}$ at the initial instant, and let both A and B be carried along with the flow. Note that $\omega(A) = k$ by the definition of the curvature: indeed, A remains tangent to the orbit for all t as it is carried with the flow with the speed $|\mathbf{f}| = 1$. On the other hand, we have $\omega(B) = 0$ at $t = 0$ since $\mathbf{f} \perp B$ and since $|\mathbf{f}| = \text{const}$. We conclude: $\omega(A) + \omega(B) = k + 0 = k$. ∎

(c) Application 2: potential fields

If the force field is conservative (such as in the Paul trap, for instance): $\mathbf{f} = -\nabla V(\mathbf{x})$ in equation (2.1),[2] so that the latter becomes

$$\ddot{\mathbf{x}} = -a\nabla V, \tag{2.10}$$

then the averaged equations (2.4) become, assuming for simplicity $\langle a\rangle = 0$:

$$\ddot{\mathbf{X}} = -\langle v^2\rangle \nabla W + \mathbf{E}, \quad \text{where } W = \tfrac{1}{2}\,\mathbf{f}^2 = \tfrac{1}{2}(\nabla V)^2. \tag{2.11}$$

Indeed, $\mathbf{f}'\mathbf{f} = (1/2)(\mathbf{f}^2)' \equiv \nabla W$.

Remark 2.4. Every isolated critical point of V is a minimum of W. Therefore, *every* isolated equilibrium of the original potential system is stabilized in the sense that every such equilibrium point is a minimum of the time-independent potential W. Note that $\mathbf{E}$ is small compared to the leading term in (2.11): $|\mathbf{E}| \approx \varepsilon^{1+(\alpha/2)}\langle v^2\rangle \ll \langle v^2\rangle$. The net effect is the attraction towards the equilibrium. The cumulative effect of $\mathbf{E}$ is discussed in §2f.

(d) Application 3: the double pendulum

Following [13], consider the double pendulum (a pendulum to whose bob another pendulum is attached), with the suspension point undergoing periodic vertical oscillations. We only consider

[2]We use the notations $V'(\mathbf{x}) \equiv \nabla V(\mathbf{x})$ interchangeably.

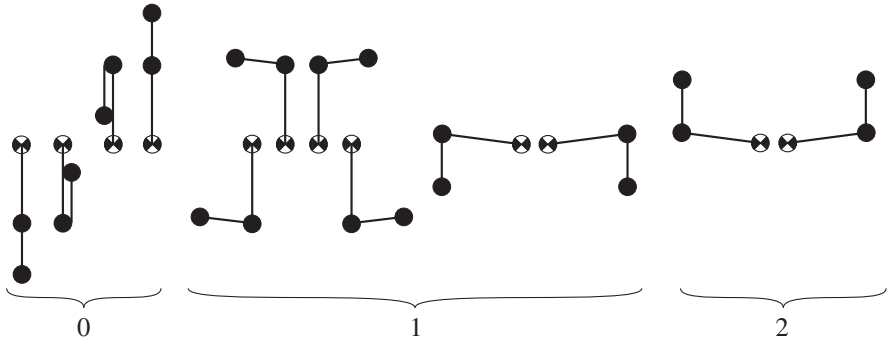

Figure 2. Morse indices of the equilibria of the averaged double pendulum.

motions confined to a vertical plane. The equations of motion are in the form slightly more general than (2.1): they come from the Lagrangian

$$L(\mathbf{x}, \dot{\mathbf{x}}, t) = \frac{1}{2}\langle \mathbf{A}(\mathbf{x})\dot{\mathbf{x}}, \dot{\mathbf{x}}\rangle - a\left(\frac{t}{\varepsilon}\right)V(\mathbf{x}), \tag{2.12}$$

where $\mathbf{A}$ is a positive definite symmetric matrix, where $\mathbf{x} = (\theta_1, \theta_2)$ with θ_i being the deflection angles from the vertical, and where $\langle \cdot, \cdot \rangle$ denotes the standard dot product in $\mathbb{R}^2$. Here, $a = -g$ minus the acceleration of the suspension point; assuming the latter to be large, we treat g as a small perturbation, omitting it altogether. This omission has no effect on the qualitative picture. We thus consider (2.12) with $\langle a \rangle = 0$. The averaged equations have the Lagrangian (modulo higher-order terms)

$$\mathcal{L}(\mathbf{X}, \dot{\mathbf{X}}, t) = \tfrac{1}{2}\langle \mathbf{A}(\mathbf{X})\dot{\mathbf{X}}, \dot{\mathbf{X}}\rangle - \langle v^2 \rangle W(\mathbf{X}), \tag{2.13}$$

where $W = (1/2)\langle \mathbf{A}^{-1}V', V'\rangle$. The potential W is a function on the torus $\mathbb{T}^2$, and we wish to count critical points of W which correspond to the equilibria of the truncated averaged system. Since V has four critical points $\mathbf{x} = (\theta_1, \theta_2) = (\pi k_1, \pi k_2)$, where $k_i \in \{0, 1\}$, W has four minima. A function on the torus with four minima must have other critical points, so that we know without any computation that there must be additional equilibrium positions for the averaged equations.

We now determine the least number of these equilibria by a topological argument. Let m_0, m_1 and m_2 be the respective numbers of minima, saddles and maxima of W. The Euler characteristic of the torus is $0 = m_0 - m_1 + m_2$. Since $m_0 =$ the number of critical points of V, we have $m_0 \geq 4$ (we assume the generic case of non-degenerate critical points). Since W must have at least one maximum, we have $m_2 \geq 1$. From this, we conclude that the number of saddles $m_1 = m_0 + m_2 \geq 4 + 1 = 5$, and thus the number of equilibria of W is at least 10. For the case of a double pendulum, we can invoke additional symmetry considerations to conclude that $m_0 + m_1 + m_2 \geq 12$; these equilibria are sketched in figure 2. For a more detailed discussion of multiple pendula, we refer to [4,9] and references therein.

(e) Application 4: a single pendulum

For the single pendulum, the above topological argument predicts two additional equilibria, figure 3; these are unstable. This is confirmed by the application of theorem 2.1. Indeed, the angle x with the upward vertical direction evolves according to

$$l\ddot{x} = (g + a(t)) \sin x, \ \langle a \rangle = 0.$$

Assume $a(t)$ to be like in (2.2); then theorem 2.1 gives the averaged truncated equation

$$l\ddot{x} = g \sin x - \frac{\langle v^2 \rangle}{l} \sin x \cos x, \tag{2.14}$$

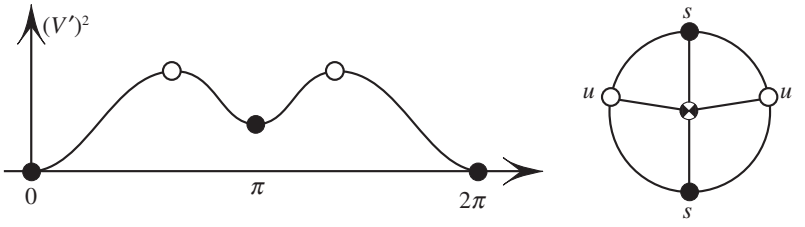

Figure 3. Four equilibria of the averaged single pendulum.

where the error terms have been removed. The effective potential $g\cos x - (1/2l)v^2\sin^2 x$ has four critical points, assuming $gl < \langle v^2\rangle$ (figure 3). For more details on the dynamics near these equilibria, we refer to [16].

(f) Error bounds

Let $\mathbf{X}$ and $\bar{\mathbf{X}}$ be the solutions of (2.11) and of the truncated equation respectively, sharing the same initial condition. The error $\mathbf{X} - \bar{\mathbf{X}}$ remains small for time $O(\varepsilon^{-(\alpha/2)})$, as follows from results in [17] applied to (2.4). For $\alpha < 0$ ('violent' vibration) this time is short and such estimates are of little use. Nevertheless, one can still obtain physically useful estimates on the energy for longer time intervals. Take, to be specific, the 'worst' case of $\alpha = -1$ so that

$$\mathbf{E} = O(\sqrt{\varepsilon}) \equiv \sqrt{\varepsilon}\mathbf{G}\left(\mathbf{x}, \dot{\mathbf{x}}, \frac{t}{\varepsilon}, \varepsilon\right), \tag{2.15}$$

where $\mathbf{G}$ is bounded when its arguments are.

Theorem 2.5 ([13]). *Fix initial conditions $\mathbf{x}_0, \dot{\mathbf{x}}_0$, and let $\mathbf{x}$ be the solution of* (2.11). *Consider the case*[3] *of $\alpha = -1$. There exist positive constants ε_0 and K independent of ε such that the 'energy'*

$$\mathcal{H} = \tfrac{1}{2}(\dot{\mathbf{x}} - v(t)\mathbf{f}(\mathbf{x}))^2 + W(\mathbf{x}).$$

satisfies

$$|\mathcal{H}(t) - \mathcal{H}(0)| \le \sqrt{\varepsilon}Kt + K\varepsilon, \quad \text{for } |t| < \frac{1}{K\sqrt{\varepsilon}}. \tag{2.16}$$

This estimate shows that the particle spends a long time in the well of the effective potential W.

The above discussion leaves open the question of stability of (2.11) for all time. In fact, for $n > 1$ such stability is virtually certain to fail due to Arnold diffusion. For the case of $n = 1$ the proof of stability for all time depends on the verification of the assumptions of the Kolmogorov–Arnold–Moser theory. There is a considerable literature by now dealing with such questions, see [18] and references therein. Using the methods developed there one can prove stability under some mild additional assumptions on V.

3. Geometrical averaging

In this section, we develop more systematically the heuristic geometrical explanation of the Stephenson–Kapitsa effect. We put this effect in a more general setting and state the rigorous results. More specifically, we point out that the ponderomotive force $-\langle v^2\rangle f'f$ in (2.4) in the case of $n = 1$ d.f. is precisely the averaged centrifugal force of a certain constraint.

The idea is to interpret

$$\ddot{x} = -a(t,\varepsilon)V'(x), \quad x \in \mathbb{R} \tag{3.1}$$

as describing the motion of a particle constrained to an oscillating curve in the plane—the simplest possible case, but still non-trivial, of geodesic motion on a vibrating manifold.

[3]For simplicity, the general case goes verbatim.

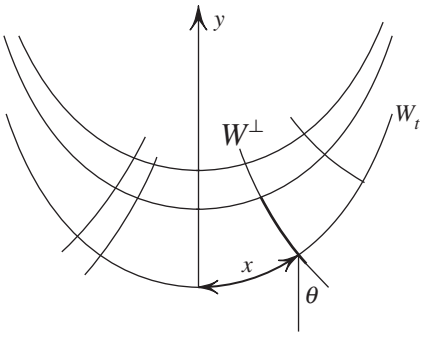

Figure 4. The family of translates W_t and the normal family $W^\perp$.

We begin by defining the curve W in $\mathbb{R}^2$ as the image of the graph $y = V(x)$ of the potential under the map

$$x \mapsto \int_0^x \sqrt{1 - V'(\sigma)^2}\, \mathrm{d}\sigma, \quad y \mapsto y \tag{3.2}$$

of the xy-plane (for this to make sense we restrict attention to the set $\{x : |V'(x)| \leq 1\}$ throughout this section.)

For instance, for $V = x^2$ the corresponding curve W is a cycloid; and for $V = \cos x$ the corresponding curve W is a circle.

Let us now subject W to oscillations in the y-direction with acceleration $a(t, \varepsilon)$, i.e. let W_t be the y-translate of W by $s(t, \varepsilon)$, where s is defined in (2.3). Finally, let $\mathcal{W}^\perp$ denote the family of curves normal to the family $\{W_t\}$.

Theorem 3.1 ([19]). *Consider a unit point mass constrained to some fixed curve $W^\perp$ from $\mathcal{W}^\perp$, and in addition to the moving curve W_t. The centrifugal force of the constraint to $W^\perp$ is precisely the ponderomotive force in the averaged equation* (2.11)*. This force is given by*

$$\langle v^2 \rangle f'(x) f(x) = \langle v^2 \rangle\, k^\perp(x)\, \sin^2 \theta, \tag{3.3}$$

where

- $v = \int a \mathrm{d}\tau$ *(the velocity of W_t in the y–direction),* $\langle v \rangle = 0$
- $k^\perp = k^\perp(x, t)$ *is the curvature of the curve $W^\perp$ at the distance x measured along W_t from the y-axis*
- $\theta = \theta(x)$ *is the angle shown in figure 4.*

We did not include gravity in the above theorem, since we wish to isolate the essential phenomenon in its simplest form and since inclusion of gravity does not give rise to any new effects.

The averaged equation (2.11), or rather its special form in the linear case, appears in Landau–Lifshitz [14]; theorem 3.1 uncovers the hidden geometry behind this result. The advantage of the geometrical reasoning, in this case, is that it allows one to guess the correct form of the averaged equations without difficulty; it is unclear how this result can be obtained otherwise without a page–long derivation (also non-rigorous) as in Landau–Lifshitz [14]. The rigorous proof is much longer and involves somewhat tedious and unrevealing algebra.

4. Non-holonomic shadows in averaging

In this section, we show that the connection between averaging and geometry goes deeper than has been described above.

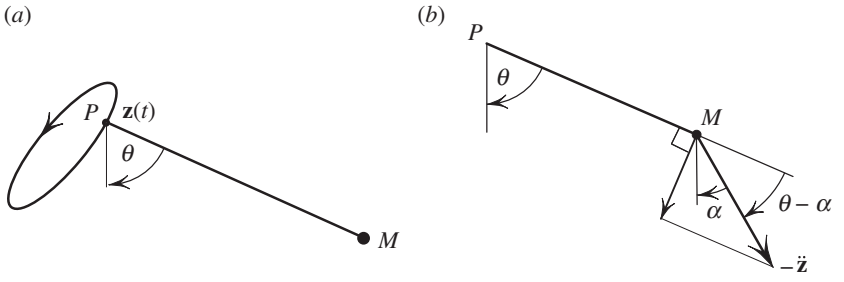

Figure 5. (*a*) A twirled pendulum and (*b*) derivation of equation (4.1).

(a) Introduction

The connection between geometry turns out to be more intimate than what has been described in the preceding sections. We illustrate this closer connection on the simplest non-trivial example, figure 5: a pendulum whose pivot $\mathbf{z}(t)$ moves periodically in a closed path. We take the path to be small and the frequency to be high: $\mathbf{z}(t,\varepsilon)=\varepsilon\mathbf{Z}(\varepsilon^{-1}t)$ (here $\mathbf{Z}(\tau)$ is a closed curve in $\mathbb{R}^2$) with $\varepsilon\ll 1$. We also ignore gravity since including it will simply add predictable terms to the equations without introducing any new phenomena.

Assuming also the presence of viscous drag in the hinge and taking the length of the pendulum to be 1, the angle θ in figure 5 satisfies

$$\ddot{\theta}+c\dot{\theta}=a(t,\varepsilon)\sin(\theta-\alpha(t,\varepsilon)), \tag{4.1}$$

where $c>0$ is the drag coefficient, $a=|\ddot{\mathbf{z}}|$ and α is the angle shown in figure 5 (right). Derivation of (4.1) is similar to the derivation of (1.8), and we give it here. We pass to the reference frame of the pivot; in this frame the mass (which we take $m=1$) is subject to the D'Alembert inertial force $-\ddot{\mathbf{z}}$; and the component of this force tangential to the unit circle is $|\ddot{\mathbf{z}}|\sin(\theta-\alpha)$, as figure 5 illustrates, confirming (4.1).

Equation (4.1) can be written more directly in terms of the pivot's acceleration $\ddot{\mathbf{z}}$:

$$\ddot{\theta}+c\dot{\theta}=\ddot{\mathbf{z}}\cdot\mathbf{F}(\theta),\quad \text{where } \mathbf{F}=\langle\sin\theta,-\cos\theta\rangle. \tag{4.2}$$

Parenthetically, this equation also governs the particle in a sinusoidal potential with time-dependent amplitude a, with a shifting phase α, and in the presence of drag.

(b) Notations

To uncover the hidden geometry of the problem we need to define three quantities $\mathcal{A},\mathcal{B}$ and $\mathcal{C}$; their geometrical meaning is explained after the definition. We let $f=f(t,\theta)$ and $g=g(t,\theta)$ be two given functions periodic in both variables, of periods 1 and 2π in t and θ respectively, and define

$$\mathcal{A}_f=\mathcal{A}_f(\theta)=\int_0^1 f'\dot{f}\,\mathrm{d}t,\quad \text{where } f'=\frac{\partial f}{\partial\theta},\ \dot{f}=\frac{\partial f}{\partial t}, \tag{4.3}$$

$$\mathcal{B}_{f,g}(\theta,t_0)=\int_0^1\left(\frac{1}{2}f^2g''-\big(f'(t,\theta)-f'(t_0,\theta)\big)fg'\right)\mathrm{d}t \tag{4.4}$$

and

$$\mathcal{C}_f(\theta,\tau)=\dot{f}\dot{f}'. \tag{4.5}$$

(i) Geometrical interpretations of $\mathcal{A}$, $\mathcal{B}$ and $\mathcal{C}$

From now on we will take $f(t,\theta)=\mathbf{Z}\cdot\mathbf{F}(\theta)$, where $\mathbf{F}$ is given in (4.2). Then $\mathcal{A}$, $\mathcal{B}$ and $\mathcal{C}$ are associated with the closed curve $\mathbf{Z}$, and have the following geometrical interpretation.

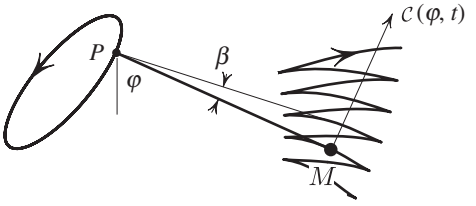

Figure 6. The non-holonomic skate, or bike. The velocity of M is constrained to the line PM. Here, $\mathcal{C}$ is the centrifugal force with which a unit point mass acts on the constraint as P.

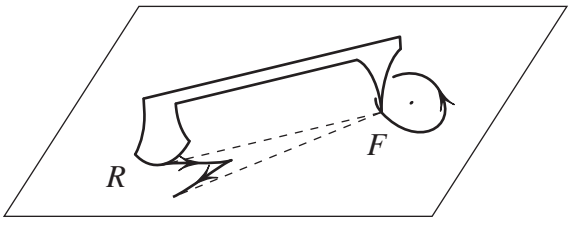

Figure 7. The Prytz planimeter.

1. $\mathcal{A}_f$ is the area enclosed by the path of $\mathbf{Z}(t)$. Indeed, $f' \equiv \mathbf{Z} \cdot \mathbf{F}' = X$ and $f \equiv \mathbf{Z} \cdot \mathbf{F} = Y$ are[4] precisely the coordinates of $\mathbf{Z}$ in the (right-handed) orthonormal frame $(\mathbf{F}', \mathbf{F})$. Thus $\mathcal{A}_f = \int_0^1 f'\dot{f}\,\mathrm{d}t = \oint X\,\mathrm{d}Y =$ area inside $\mathbf{Z}$, as claimed.
2. Let us take $g = \dot{f}$. Then $\mathcal{B}_{f,\dot{f}}(\theta, t_0) = \bar{x}\mathcal{A}_f$, where $\bar{x}$ is the distance from the centroid of the domain $\mathbf{D}$ enclosed by the path of $\mathbf{Z}$ to the line through $\mathbf{Z}(t_0)$ in the direction $-\mathbf{F}(t_0)$. In other words, $\mathcal{B}_{f,\dot{f}}(\theta, t_0)$ is the torque around the axis through $\mathbf{Z}(t_0)$ in the direction $-\mathbf{F}(t_0)$ of the uniformly distributed force applied to the lamina $\mathbf{D}$, perpendicular to the lamina. Indeed, $f'' = -f$ and (4.4) with $g = \dot{f}$ yields
$$\mathcal{B}_{f,\dot{f}} = \int_0^1 \left(-\frac{1}{2}f^2\dot{f} - (f' - f_0')f\dot{f}'\right)\mathrm{d}t = -\oint (X - X_0)Y\,\mathrm{d}X = -\iint_{\mathbf{D}} (X - X_0)\,\mathrm{d}X\,\mathrm{d}Y = \bar{x}\mathcal{A}_f, \tag{4.6}$$
as claimed.
3. To endow $\mathcal{C}_f(\theta, \tau)$ with a physical meaning, we impose an artificial constraint on the pendulum's bob by restricting its velocity the direction of the rod; in other words, we are replacing the pendulum with a non-holonomically constrained 'skate' PM, where M's velocity is constrained to the line PM, figure 6. With such constrained imposed, $\mathcal{C}_f(\theta, \tau)$ *is the centrifugal acceleration of* M; in particular $\mathcal{C}_f(\theta, \tau) = kv^2$, where $k = k(\theta, \tau)$ is the curvature of the (constrained) M's path, while $v = v(\theta, \tau)$ is M's speed. Indeed, recall that the centrifugal acceleration of a moving point is the product of the rate of rotation of its velocity vector and of its speed. But $\mathcal{C}_f(\theta, t) = \dot{f}\dot{f}' = (\dot{\mathbf{Z}}(t) \cdot \mathbf{F}(\boldsymbol{\theta}))(\dot{\mathbf{Z}}(t) \cdot \mathbf{F}'(\boldsymbol{\theta}))$ is precisely such a product.

(c) A non-holonomic system

In this section, we point out that the quantities $\mathcal{A}$, $\mathcal{B}$ and $\mathcal{C}$ appear in a non-holonomically constrained system: the 'skate', also known as the Prytz planimeter, depicted in figure 7. We first describe the device and then show how it gives rise to $\mathcal{A}$, $\mathcal{B}$ and $\mathcal{C}$.

[4]Here $' = (\mathrm{d}/\mathrm{d}\theta)$ and $\dot{} = (\mathrm{d}/\mathrm{d}t)$.

The Prytz planimeter is a mechanical device invented by Holger Prytz about 1875 to measure areas, as mentioned in [20], see also references therein, e.g. [21,22]. The hatchet-shaped end R helps prevent sideslip; the same effect can be achieved by attaching a wheel oriented along RF at R, like the rear wheel of a scooter. Formally speaking, the planimeter is a rigid segment RF whose end F (front) travels along a prescribed path, while the velocity of its 'rear' end R is constrained to line up with the segment. If F executes a closed path, returning to its initial position, R ends up in the new position, i.e. RF ends up rotated through a certain angle. For small paths, in the leading order, this angle is proportional to the area of the enclosed by the path, and is independent of the initial orientation. We now make it more precise.

(i) Planimeter's equations of motion

Let θ be the angle formed by the segment RF with the positive x-axis, and let $\mathbf{z}(t) = \mathbf{z}(t+1)$ be a parameterization of the closed path K traced out by the tracer F. The no-slip constraint of the velocity of the slider R amounts to

$$\dot{\theta} = \dot{\mathbf{z}} \cdot \mathbf{F}(\theta), \tag{4.7}$$

where $\mathbf{F}$ is the same as in (4.2). To state the asymptotic result, we consider a rescaling of $\mathbf{Z}$:

$$\mathbf{z}(t) = \varepsilon \mathbf{Z}(t),$$

so that equation (4.7) takes form

$$\dot{\theta} = \varepsilon \dot{\mathbf{Z}}(t) \cdot \mathbf{F}(\theta), \tag{4.8}$$

The following theorem is a restatement of the theorem due to Prytz, see also Foote [20].

Theorem 4.1 ([23]). *Let $\theta = \theta(t)$ be a solution of (4.8). One has*

$$\theta(t_0 + 1) - \theta(t_0) = \varepsilon^2 \mathcal{A}_f + \varepsilon^3 \mathcal{B}_{f,\dot{f}}(\theta, t_0) + O(\varepsilon^4), \tag{4.9}$$

where $f(t, \theta) = \dot{\mathbf{Z}}(t) \cdot \mathbf{F}(\theta)$ and where $\mathcal{A}$, $\mathcal{B}$ and $\mathcal{C}$ are defined in (4.3)–(4.5).

Note that the first term on the right is independent of the initial orientation θ_0.

(d) The averaging theorem for the twirled pendulum

The next theorem shows that the shadow of the non-holonomic constraint of the 'bike' arises in the averaged form of the rapidly twirled pendulum. The twirled pendulum's motion is governed by (4.2) where we assume

$$\mathbf{z}(t, \varepsilon) = \varepsilon \mathbf{Z}\left(\frac{t}{\varepsilon}\right),$$

and where $\mathbf{Z}$ is a smooth (C^5) periodic function of period 1.

Theorem 4.2 ([23]). *There exists a change of variables $\theta = \varphi + \varepsilon g(\varphi, t, \varepsilon)$ with $g(\varphi + 2\pi, t, \varepsilon) = g(\varphi, t + \varepsilon, \varepsilon) = g(\varphi, t, \varepsilon)$, such that equations (4.1)–(4.2) is transformed into*

$$\ddot{\varphi} + c\dot{\varphi} = \overline{\mathcal{C}}_f(\varphi) + \varepsilon \left(c\overline{\mathcal{A}}_f(\varphi) + \overline{\mathcal{B}}_{f,\dot{f}}(\varphi) \right) + \varepsilon^2 R(\varphi, t, \varepsilon), \tag{4.10}$$

where $\mathcal{C}$, $\mathcal{A}$ and $\mathcal{B}$ are defined in (4.5), (4.3) and (4.4), where $f(t, \theta) = \mathbf{Z} \cdot \mathbf{F}$ and where the bar denotes the time average.

We conclude that the three quantities associated with the non-holonomic Prytz planimeter appear also in the twirled pendulum (the term $\mathcal{C}$ appearing in (4.10) is also the force of non-holonomic constraint on the slider R if it were endowed with a unit mass, figure 6). In other words, we find that a non-holonomic system hides in the shadow of the holonomic one in the case of rapid forcing as specified here.

Remarks.

1. The forcing term in (4.2) is $O(\varepsilon^{-1})$, the 'ponderomotive' term $\mathcal{C}$ is $O(1)$, and the next two terms are $O(\varepsilon)$.
2. The area term in (4.10) arises only if the drag coefficient $c \neq 0$.

(e) Applications of the twirled pendulum.

(i) Feynman's ratchet

As the simplest interesting example, we consider the particle in $\mathbb{R}$ subject to the sliding potential $V(\theta, t) = -(A/\varepsilon)\cos(\theta - t/\varepsilon)$; the motion is governed by the equation of 'twirled pendulum' without gravity:

$$\ddot{\theta} + c\dot{\theta} = A\varepsilon^{-1}\sin\left(\theta - \frac{t}{\varepsilon}\right), \tag{4.11}$$

a special case of (4.1) with $a(t, \varepsilon) = A/\varepsilon$, $\alpha(t, \varepsilon) = t/\varepsilon$, with $\varepsilon = \omega^{-1}$. We assume $\omega \gg 1$, i.e. the rapidly sliding potential with large amplitude. According to theorem 4.2, the averaged equation for the particle in the Feynman ratchet is given by

$$\ddot{\varphi} + c\dot{\varphi} = \varepsilon c\pi A^2 + o(\varepsilon).$$

A particle in such a potential will, to the leading order in ε, undergo drift with speed

$$v_{\text{drift}} = \varepsilon\pi A^2,$$

independent of the drag coefficient c, provided $c > 0$ – indeed, when matching the drag $c\dot{\varphi}$ to the forcing $\varepsilon c\pi A^2$ the drag coefficient cancels out. Interestingly, although the drag is responsible for the presence of drift, the speed of the drift is independent of the drag coefficient. The explanation of this seeming discontinuity lies in the fact that as $c \to 0$, the time it takes to approach v_{drift} approaches infinity.

(ii) A bead on a rigid hoop

As another application of theorem 4.2 we consider a point mass constrained to a rigid hoop in $\mathbb{R}^2$. The particle is subject to drag proportional to the speed of sliding along the hoop. No additional forces, apart from the constraint and the drag, act on the bead.

Adiabatic motion of this system in the conservative (i.e. the drag-free) case has been studied by Berry & Hannay [24], who showed that as the hoop undergoes one slow revolution around a fixed point, the bead running with speed $O(1)$ around the hoop ends up shifted, compared to its twin on a stationary hoop, by the arclength $A/2\pi L$ where A and L are respectively the area and the length of the hoop. In this section, we demonstrate a different holonomy effect in the 'opposite' asymptotic case, that of a rapidly vibrating hoop, *and* in the presence of friction. Again, as in the previous case, we will see an associated non-holonomic system as the singular limit of the original holonomic system.

Equations of motion. Consider a smooth closed curve (the hoop) $\mathbf{r} : \mathbb{R} \mapsto \mathbb{R}^2$ parameterized by the arclength s, and let this undergo oscillatory translational motion: $\mathbf{r}(s, t) = -\mathbf{z}(t) + \mathbf{r}(s)$; the negative sign is used for later convenience. The hoop thus oscillates in a closed path, undergoing parallel translations by $-\mathbf{z}$. We assume small-amplitude, high-frequency motions: $\mathbf{z}(t, \varepsilon) = \varepsilon\mathbf{Z}(t/\varepsilon)$. The equation of motion of the bead constrained to the hoop is

$$\ddot{s} + c\dot{s} = \mathbf{a} \cdot \mathbf{T}(s), \tag{4.12}$$

where $\mathbf{a}(t) = \ddot{\mathbf{z}}$ and $\mathbf{T} = \mathbf{r}'(s)$ is the unit tangent vector.

Remark 4.3. The twirled pendulum is a special case in which the hoop is a circle.

With $\mathbf{z} = \varepsilon \mathbf{Z}(t/\varepsilon)$, theorem 4.2 applies: there exists a transformation $s = \sigma + \varepsilon g(\sigma, t, \varepsilon)$ turning equation (4.12) into (4.10). The truncated averaged equations take form

$$\ddot{\sigma} + c\sigma = \overline{\kappa^{\perp} u^2} + \varepsilon \left(\kappa \mathcal{A} + \overline{\mathcal{B}_{f,\ddot{f}}} \right), \tag{4.13}$$

where

— $\kappa^{\perp} = \kappa^{\perp}(\sigma, t)$ is the curvature of the curve normal to the family of translates $\mathbf{r}(\sigma) - \mathbf{z}(t)$.
— $u = \dot{\mathbf{z}} \wedge \mathbf{r}'$ is the normal velocity of the hoop;
— $\mathcal{A}$ is the area enclosed by the curve $\mathbf{z}(t)$;
— $\kappa(\sigma) = |\mathbf{r}''(\sigma)|$ is the curvature of the hoop as the function of the arclength.

5. Geodesics on vibrating surfaces

So far, we have discussed the motion of a particle in $\mathbb{R}^n$, as well as of particles constrained to moving curves. In this section, we describe a generalization to vibrating constraints to higher dimension, considering the simplest case of 2 d.f. Specifically, we consider the motion of a particle confined to a moving surface in $\mathbb{R}^3$ given by

$$\varphi(x, y, z) - s(t, \varepsilon) = 0, \tag{5.1}$$

where $s = \varepsilon s_1(t/\varepsilon)$, $s_1(\tau + 1) = s_1(\tau)$ is a periodic function and $\varepsilon > 0$. We assume that no forces, apart for the surface constraints, act on the particle. In other words, we study the classical problem of geodesic motion on surfaces, but with an added twist: the surface vibrates or deforms rapidly. We would like to understand the averaged effect of this vibration. As before, we consider the small-amplitude high-frequency case. We start with a heuristic derivation of the averaged equations of motion, and follow it by the rigorous statement.

(a) Averaged equations of motion

Consider the family of surfaces $\mathcal{S}$ in $\mathbb{R}^3$ (5.1) parametrized by t. Assuming that the gradient $\nabla\varphi = \varphi' \neq 0$, the family $\mathcal{F}^{\perp}$ of curves normal to the family $\mathcal{S}$ is well defined. Let $k = k(\mathbf{R})$ be the curvature of a curve from $\mathcal{F}^{\perp}$ passing through a point $\mathbf{R} \in \mathbb{R}^3$, and let $\mathbf{N} = \mathbf{N}(\mathbf{R})$ be the principal normal vector to this curve. Finally, let v be the normal speed of the moving surface (5.1), i.e. let $v = \dot{s}/|\varphi'|$.

According to the following theorem, the vibration of the surface gives rise to the ponderomotive force tangential to the surface, and equal to the centrifugal force of a *non-existent constraint:* the constraint to a curve from the family $\mathcal{F}^{\perp}$.

Theorem 5.1 ([25]). *There exists a time-dependent transformation* $\mathbf{r} \mapsto \mathbf{R}$

$$\mathbf{r} = \mathbf{R} + \mathbf{h}(\mathbf{R}, t, \varepsilon) \tag{5.2}$$

which decomposes the motion $\mathbf{r}$ *into the average motion* $\mathbf{R}$ *and the fluctuation* $\mathbf{h} = O(\varepsilon)$, *such that* $\mathbf{R}$ *satisfies*

$$\ddot{\mathbf{R}} = -(\varphi''\dot{\mathbf{R}}, \dot{\mathbf{R}})\boldsymbol{\Phi} - k\langle v^2 \rangle \mathbf{N} + \mathbf{E}, \tag{5.3}$$

where $\mathbf{E} = o(1)$ *and where* $\boldsymbol{\Phi}$ *is the rescaled gradient*

$$\boldsymbol{\Phi} = \frac{\varphi'}{|\varphi'|^2} \quad \text{and} \quad \varphi' \equiv \nabla\varphi. \tag{5.4}$$

Remark 5.2. The truncated averaged equation

$$\ddot{\mathbf{R}} = -(\varphi''\dot{\mathbf{R}}, \dot{\mathbf{R}})\boldsymbol{\Phi} - k\langle v^2 \rangle \mathbf{N} \tag{5.5}$$

leaves the tangent bundle of any surface $S := \{\varphi = \text{const.}\}$ invariant: for any solution $\mathbf{R}(t)$ of equation (5.5), if $\mathbf{R}(t) \in S$ and $\dot{\mathbf{R}}(t) \in T_{\mathbf{R}(t)}S$ for some t, then the same is true for all t.

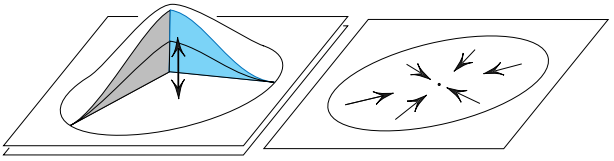

Figure 8. The vibration of a surface patch creates an effective potential force attracting towards the point of maximal amplitude. (Online version in colour.)

Remark 5.3. The first term on the right in (5.3) is the centripetal force of constraint to a *stationary* surface $\varphi = \text{const}$.

(i) A heuristic derivation of equation (5.3)

Since $s(t) = \varepsilon s_1(t/\varepsilon)$ is rapidly oscillating, we expect the particle to move primarily in the normal direction to the surface, i.e. along one of the curves from the normal family. If the particle were actually constrained a normal curve, the *centripetal* force of constraint would arise, namely $kv^2\mathbf{N}$, with the average $k\langle v^2\rangle\mathbf{N}$ over the period ε. Now let us remove our non-existent constraint, and thus the centripetal force; the released particle then should behave as if the opposite force $-k\langle v^2\rangle\mathbf{N}$ were acting on it. This explains the last term in (5.5).

There is an striking contrast between the brevity of the above heuristic argument and the much greater length of a rigorous proof of (5.3) (found in [25]). The heuristic argument also reveals a geometric aspect of the averaged equations obtained by a formal argument. This geometric form looks quite different from (5.3), and it is not clear how the geometric significance of these averaged equations could be discovered by other means. In fact, the geometrical form (5.3) of the averaged equations was arrived at before the rigorous proof of it was given in [25]. It would be of interest to convert the heuristic argument into a rigorous proof, thereby replacing the normal form-based argument in which the underlying geometry remains hidden.

(ii) An illustration

Consider the time-dependent surface with a 'vibrating bump', as shown in figure 8. According to the above, the effect of this vibration is to create a potential well, i.e. an effective force attracting to a potential minimum inside the vibrating patch.

6. Ponderomotive magnetism

Most problems addressed so far were special cases of the Newtonian system

$$\ddot{\mathbf{x}} = -\nabla V(\mathbf{x}, t).$$

It turns out that if, unlike in prior sections, ∇V exhibits some rotation in time (for fixed x and as a function of t), then a new effect arises. This section summarizes some results from [26].

(a) Some background

It is a fundamental fact of nature that a changing electric field creates a magnetic field. Interestingly, a superficially analogous effect arises in mechanics: in a rapidly changing force field a particle acts as if it were subject to Lorentz force. This happens, for example, when a point mass is placed in the rapidly rotating saddle potential [27]. The *ponderomotive Lorentz force*, a term introduced in [26], seems to be a fitting name for this magnetic-like force, since it is given by the same mathematical expression as the Lorentz force (where the 'magnetic field' is given in

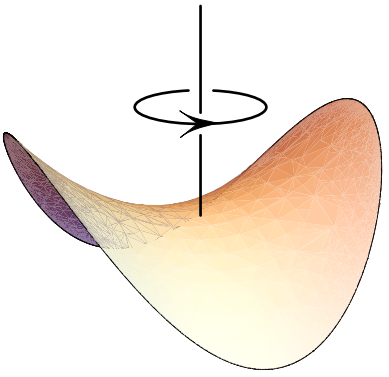

Figure 9. A rotating saddle potential. (Online version in colour.)

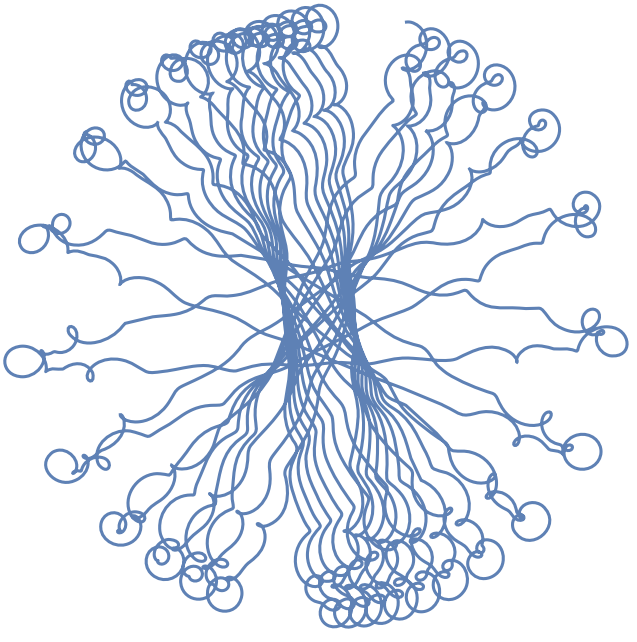

Figure 10. The motion of a particle in a potential which includes both vibrating and rotating terms. (Online version in colour.)

terms of the potential). This force does not appear in the problems with separated time and space dependence discussed in §2—but for more general time-dependence it occurs 'generically'.[5]

A long list of examples from physics which fall in the class studied in this section can be found in [27,28]. Historically, perhaps the first such example was analysed by Brouwer [29] (of the Bohl–Brouwer fixed point theorem). Brouwer actually considered a particle sliding on a rotating saddle surface in the presence of gravity, as in figure 9. The linearized equations near the equilibrium, however, are the same as those describing a particle in a rotating saddle potential.

There seems to be no mention of this magnetic-like force in the literature apart from [26,30–32]. Figure 10 illustrates a typical motion in the presence of some rotation in the potential. In addition to the 'wiggling' motion the particles undergo a certain precession-like motion. The latter turns out to be a manifestation of the hidden 'ponderomotive magnetism' which is described in theorems 6.1 and 6.2 below (and in more detail in [26]).

[5]The precise meaning of this is clear from theorem 6.2.

(b) The main result

Following [26], we consider the motion of a particle in a rapidly oscillating potential,

$$\ddot{x} = -\nabla U\left(x, \frac{t}{\varepsilon}\right), \quad x \in \mathbb{R}^n, \tag{6.1}$$

where the gradient is taken with respect to x, the function U is periodic in the second variable:

$$U(x,\tau) = U(x,\tau+1),$$

and where ε is a small parameter. Examples of this include the separable case $U(x,t) = a(t)V(x)$, the rotating saddle, and much more.

For future reference, we note that (6.1) is equivalent to the Hamiltonian system with the Hamiltonian

$$H(x,p,t/\varepsilon) = \frac{1}{2}p^2 + U\left(x, \frac{t}{\varepsilon}\right). \tag{6.2}$$

The main theorem, to be stated shortly, refers to the three temporal antiderivatives of U ('velocity', 'position' and 'absement' potentials):

$$V(x,\tau) = \int [U(x,\tau) - \overline{U}(x)]\,\mathrm{d}\tau, \quad S(x,\tau) = \int V(x,\tau)\,\mathrm{d}\tau,\ A(x,\tau) = \int S(x,\tau)\,\mathrm{d}\tau, \tag{6.3}$$

where $\overline{U} = \overline{U}(x)$ denotes the time average of U over one temporal period, and where each of the indefinite integrals is chosen to have zero time average:

$$\overline{V} = \overline{S} = \overline{A} = 0.$$

For the sake of brevity, the x-derivative of a function $f\colon \mathbb{R}^n \to \mathbb{R}$ will be denoted by a prime ($'$) rather than by ∇. Similarly, the Hessian will be denoted by two primes, so that

$$U' = \nabla U, \quad U'' = \nabla^2 U, \text{ etc.}$$

The following two theorems show, in particular, the appearance of the ponderomotive Lorentz force.

Theorem 6.1 ([26]). *Assume that the potential U in (6.1) is of class C^3 in x and continuous in t. For any fixed ball in the* phase space *$\mathbb{R}^{2n}$ there exists $\varepsilon_0 > 0$ such that for each positive $\varepsilon < \varepsilon_0$ there is a time-parameterized family of symplectic transformations*

$$\psi^\tau = \psi_\varepsilon^\tau\colon (x,p) \mapsto (X,P)$$

defined on the ball and periodic of period one in τ, such that the time-dependent transformation $\psi^{t/\varepsilon}$ turns the system with the Hamiltonian (6.2) into the system with the Hamiltonian

$$K(X,P,t/\varepsilon) = \frac{1}{2}P^2 + \overline{U} + \frac{\varepsilon^2}{2}\overline{V'\cdot V'} - \varepsilon^3\left(\overline{S''V'}\cdot P\right) + O(\varepsilon^4), \tag{6.4}$$

which is time-independent to third order.

For the Newtonian formulation (6.1), we have the following, recalling the notation from (6.3).

Theorem 6.2 ([26]). *Any solution $x = x(t)$ of (6.1) has the associated guiding centre*

$$X = x + \varepsilon^2 S'\left(x, \frac{t}{\varepsilon}\right) - 2\varepsilon^3 A''\left(x, \frac{t}{\varepsilon}\right)\dot{x} + O(\varepsilon^4) \tag{6.5}$$

which behaves as a charged particle subject to potential and magnetic forces:

$$\ddot{X} = -\overline{U}'(X) - \varepsilon^2 W'(X) + \varepsilon^3 B(X)\dot{X} + O(\varepsilon^4), \tag{6.6}$$

where $W = (1/2)\overline{V'\cdot V'}$ and B is the skew-symmetric matrix given by $B = (b')^T - b'$, with $b = \overline{S''V'}$.

We do not specify the $O(\varepsilon^4)$ term in (6.5) for the sake of simplicity; it can easily be obtained from the proof if desired.

Remark 6.3. The term $B(X)\dot{X}$ in (6.6) can be interpreted as the force produced by a magnetic field. In dimension $n=2$, the strength of this field (normal to the plane) is $2\,\mathrm{curl}\,b$, where curl denotes the scalar curl in $\mathbb{R}^2$.

Remark 6.4. Although the original system (6.1) is fully nonlinear, its averaged counterpart (6.6) is, to leading order, linear in the velocity.

(c) Applications

The examples of this section give particularly simple illustrations of theorem 6.2. These are:

1. the rotating saddle potential;
2. the purely oscillatory potential;
3. a potential whose graph is a rotating ruled surface.

(i) The rotating saddle

In this special case of physical interest, as described in [28], the potential U is quadratic and rapidly rotating, i.e. of the form

$$U = U_0\left(R^{-1}\left(\frac{t}{\varepsilon}\right)x\right),$$

where $U_0(x) = (x_1^2 - x_2^2)/2$, $x = (x_1, x_2) \in \mathbb{R}^2$, and

$$R(\tau) = \begin{pmatrix} \cos\tau & -\sin\tau \\ \sin\tau & \cos\tau \end{pmatrix}$$

is the counterclockwise rotation. In this case, the transformation (6.5) takes the form

$$X = x - \varepsilon^2 Q\left(\frac{t}{\varepsilon}\right)(x - 2\varepsilon J\dot{x}) + O(\varepsilon^5)$$

with $\varepsilon = (2\omega)^{-1}$ (note the absence of the ε^4-term) and with

$$Q(\tau) = \begin{pmatrix} \cos\tau & \sin\tau \\ \sin\tau & -\cos\tau \end{pmatrix} \quad \text{and} \quad J = \begin{pmatrix} 0 & -1 \\ 1 & 0 \end{pmatrix},$$

and the averaged equation becomes

$$\ddot{X} = -\varepsilon^2 X - 2\varepsilon^3 J\dot{X} + O(\varepsilon^4),$$

in agreement with the result in [30] (it should be noted that the ε in that paper is twice the present ε).

(ii) The purely oscillatory potential

Another special case of physical importance is

$$\ddot{x} = -a\left(\frac{t}{\varepsilon}\right)U'(x), \tag{6.7}$$

where a is real-valued and periodic. This equation describes, among other things, the motion of charged particles in the Paul trap [33], in which an electric field is generated by oscillating voltages on electrodes. The inverted pendulum with oscillating suspension is another example. The averaged equation (6.6) becomes (omitting some algebra)

$$\ddot{X} = -\bar{a}\,U'(X) - \varepsilon^2\,\overline{v^2}\,U''(X)U'(X) + O(\varepsilon^4),$$

where $v(\tau) = \int a(\tau)\,\mathrm{d}\tau$ with $\bar{v} = 0$. Note that the cubic terms corresponding to the 'magnetic' effect vanish in this case. This is a refinement of the result of theorem 2.1, where the cubic terms were not addressed.

(iii) A rotating ruled surface and a magnetic dipole

Consider the potential U whose graph is a rotating ruled surface:

$$U(x,\tau) = h(\theta - \tau),$$

where θ is the polar angle of x, and h is a smooth 2π-periodic function. Such a potential has a singularity at the origin, and so we apply our averaging theorem to the complement of a neighbourhood of the origin. Theorem 6.2 in this case yields averaged equations, after some manipulations (see [26]):

$$\ddot{X} = \varepsilon^3\, \bar{h}\, \frac{1}{|X|^3} J\dot{X} + O(\varepsilon^4), \quad \text{where } \bar{h} = \frac{1}{2\pi}\int_0^\pi h(\theta)\, \mathrm{d}\theta.$$

The 'magnetic field' strength $\varepsilon^3\, \bar{h}/|X|^3$ falls off as the inverse cube of the distance to the origin-precisely as if a magnetic dipole with the axis normal to the plane were present at the origin!

Open problem. To conclude we point out that no geometrical explanation of ponderomotive magnetism is available at present, and that it would be of great interest to find such an explanation. It perhaps should be mentioned that a geometrical explanation of 'magnetism' is available in a different problem with analogous flavour: the motion of a *spinning* disc constrained to be tangent to a surface [34]. In that problem, the tangency point of the disc with the surface behaves as if it were a charged particle sliding on the surface and subject to the Lorentz force in the magnetic field normal to the surface of strength equal to Gaussian curvature of the surface, and with the particle's charge equal to the disc's angular momentum around its axis. Further details can be found in the last-mentioned reference.

Data accessibility. This article does not contain any additional data.

Competing interests. I declare I have no competing interests.

Funding. Partially supported by NSF grant no. DMS-9704554.

Acknowledgements. The author is grateful to two anonymous referees for some very helpful comments which helped improve the exposition.

References

1. Stephenson A. 1908 On a new type of dynamical stability. *Manch. Mem.* **52**, 1–10.
2. Kapitsa PL. 1965 Dynamical stability of a pendulum when its point of suspension vibrates. Collected Papers by P.L. Kapitsa, vol. II, pp. 714–725. London, UK: Pergamon Press.
3. Acheson DJ. 1993 A pendulum theorem. *Proc. R. Soc. Lond. A* **443**, 239–245. (doi:10.1098/rspa.1993.0142)
4. Acheson DJ, Mullin T. 1993 Upside-down pendulums. *Nature* **366**, 215–216. (doi:10.1038/366215b0)
5. Bullo F. 2002 Averaging and vibrational control of mechanical systems. *SIAM J. Control Optim.* **41**, 542–562. (doi:10.1137/S0363012999364176)
6. Kapitsa PL. 1965 Pendulum with a vibrating suspension. Collected Papers by P.L. Kapitsa, vol. II, pp. 726–737. London, UK: Pergamon Press.
7. King RE. 1965 Inverted pendulum. *Am. J. Phys.* **33**, 855. (doi:10.1119/1.1971009)
8. Bellman R, Bentsman J, Meerkov SM. 1986 Vibrational control of nonlinear systems: vibrational stabilizability. *IEEE Trans. Autom. Control* **31**, 710–724. (doi:10.1109/TAC.1986.1104384)
9. Baillieul J, Weibel S, Kaper T. 1997 Global dynamics of a rapidly forced cart and pendulum. *Nonlinear Dyn.* **13**, 131–170. (doi:10.1023/A:1008248704427)
10. Feynman R. 1965 *The Feynman lectures on physics*. Reading, MA: Addison-Wesley.
11. Arnold VI. 1992 *Ordinary differential equations*. Berlin, Germany: Springer.
12. Christofilos N. 1953 Science and the citizen. *Sci. Am.* **188**, 45–46.
13. Levi M. 1999 Geometry and physics of averaging with applications. *Physica D* **132**, 150–164. (doi:10.1016/S0167-2789(99)00022-6)
14. Landau LD, Lifshitz EM. 1976 *Course of theoretical physics*, vol. 1 (Mechanics). Oxford, UK: New York, NY: Pergamon Press.

15. Bogoliubov NN, Mitropolskii YA. 1961 *Asymptotic methods in the theory of non-linear oscillations*. New York, NY: Gordon and Breach.
16. Hoveijn I, Broer HW, van Noort M. 1998 A reversible bifurcation analysis of the inverted pendulum. *Physica D* **112**, 50–63. (doi:10.1016/s0167-2789(97)00201-7)
17. Murdock JA. 1991 *Perturbation: theory and methods*. Philadelphia, PA: SIAM.
18. Levi M, Zehnder E. 1995 Boundedness of solutions for quasiperiodic potentials. *SIAM J. Math. Anal.* **26**, 1233–1256. (doi:10.1137/S0036141093249079)
19. Levi M. 1998 Geometry of Kapitsa's potentials. *Nonlinearity* **11**, 1365–1368. (doi:10.1088/0951-7715/11/5/011)
20. Foote RL. 1998 Geometry of the prytz planimeter. *Rep. Math. Phys.* **42**, 249–271. (doi:10.1016/S0034-4877(98)80013-X)
21. Murray FJ. 1961 *Mathematical machines*. Analog Devices, vol. 2. New York, NY: Columbia University Press.
22. Pedersen O. 1987 The prytz planimeter, from ancient omens to statistical mechanics. (eds JL Berggren, BR Goldstein). Copenhagen, Denmark: University Library.
23. Levi M, Weckesser W. 2002 Non-holonomic systems as singular limits for rapid oscillations. *Ergodic Theory Dyn. Syst.* **22**, 1497–1506. (doi:10.1017/S0143385702001098)
24. Berry MV, Hannay JH. 1988 Classical non-adiabatic angles. *J. Phys. A: Math. Gen.* **21**, L325–L331. (doi:10.1088/0305-4470/21/6/002)
25. Levi M, Ren Q. 2005 Geodesics on vibrating surfaces and the curvature of the normal family. *Nonlinearity* **18**, 2737–2743. (doi:10.1088/0951-7715/18/6/017)
26. Cox G, Levi M. 2017 Magnetic terms in averaged hamiltonian systems. (https://arxiv.org/abs/1707.04970).
27. Kirillov O, Levi M. 2016 Rotating saddle trap as foucault's pendulum. *Am. J. Phys.* **84**, 26–31. (doi:10.1119/1.4933206)
28. Kirillov ON. 2003 *Nonconservative stability problems of modern physics*. Berlin, Germany: De Gruyter.
29. Brouwer LEJ. 1918 Beweging van een materieel punt op den bodem eener draaiende vaas onder den invloed der zwaartekracht. *N. Arch. v. Wisk.* **2**, 407–419.
30. Kirillov O, Levi M. 2017 A coriolis force in an inertial frame. *Nonlinearity* **30**, 1109–1119. (doi:10.1088/1361-6544/aa59a0)
31. Shapiro VE. 1998 The gyro force of high-frequency fields lost by the concept of effective potential. *Phys. Lett. A* **238**, 147–152. (doi:10.1016/S0375-9601(97)00896-7)
32. Shapiro VE. 2001 Rotating class of parametric resonance processes in coupled oscillators. *Phys. Lett. A* **290**, 288–296. (doi:10.1016/S0375-9601(01)00693-4)
33. Paul W. 1990 Electromagnetic traps for charged and neutral particles. *Rev. Mod. Phys.* **62**, 531–540. (doi:10.1103/RevModPhys.62.531)
34. Cox G, Levi M. 2018 Gaussian curvature and gyroscopes. *Commun. Pure Appl. Math.* **71**, 938–952. (doi:10.1002/cpa.21731)